Detection of terminal mismatches on DNA duplexes with fluorescent oligonucleotides†

Ulysse Asseline,* Marcel Chassignol, Yves Aubert and Victoria Roig

Received 15th February 2006, Accepted 9th March 2006
First published as an Advance Article on the web 31st March 2006
DOI: 10.1039/b602262f

This paper describes the design of terminal-mismatch discriminating fluorescent oligonucleotides (TMDFOs). The method is based on the use of sets of oligo-2′-deoxyribonucleotide probes linked *via* their 5′-ends, and varying-sized flexible polymethylene chains, to thiazole orange, with the linker being attached to the benzothiazole moiety. The sequence of each set of labelled probes was identical and complementary to the sequence to be analyzed on the single-stranded nucleic acid target except at the interrogation position, located at the 5′-end of the probes in a position adjacent to the attachment site of the label, where each of the four nucleic bases were incorporated. This work allowed the selection of probes showing, upon their hybridization with the target sequence, good discrimination between the matched and the mismatched duplexes under non-stringent conditions, with the mismatched duplexes being more fluorescent than the perfectly matched ones.

Introduction

Ever since the post genome era, there is an ever-increasing demand for sequence-selective DNA analysis including the possibility of detecting single-nucleotide changes.[1–5] Among the methods reported, those using fluorescent oligonucleotides (FONs) have the potential to simplify nucleic acid analyses if the fluorescent signal emission exhibit drastic changes when the FONs hybridize with their target sequences.[6–8] Over the past few years, FONs able to discriminate perfectly matched duplexes from mismatched ones have been designed for single nucleotide polymorphism analysis.[9–23] They include the use of modified nucleosides,[9–11] the linkage of fluorophores such as pyrene,[12–18] phenanthroline,[19] phenanthridinium[20] and fluorene[21] at different positions on the oligonucleotidic backbone. Thiazole orange, as a base surrogate, was also used in peptide nucleic acids.[22,23] The bases on the complementary strands could be fluorometrically read without separation and washing. These methods have been successful in discriminating between perfectly matched duplexes and those containing mismatches when the latter were located at internal positions of the duplexes. Nevertheless, there is still a need for the development of simple methods able to detect terminal mismatches on DNA duplexes. Thus, even for short duplexes, the presence of terminal mismatches lowers the UV-melting point by only a few degrees and the free energy of binding by <1 kcal mol^{-1}. This is less than the variation in the binding constants between strands with different sequences and C : G/T : A contents.[24,25] For these reasons, it is difficult to find stringent conditions allowing terminal mismatch detection in a high throughput analysis involving a great number of parallel hybridizations with arrays of oligonucleotides either in homogeneous assays or immobilized on chips. Along these lines, an interesting work showed that mismatch discrimination at the terminus can be improved by the appendage of different non-nucleosidic molecular "caps" resulting in an increase in the stability difference between the matched and mismatched duplexes.[26–28] We now report the design of terminal mismatch discriminating fluorescent oligonucleotides (TMDFOs). These probes are 5′-fluorescently labelled oligo-2′-deoxyribonucleotides (ODNs) able to detect terminal mismatched base-pairs on DNA duplexes under non-stringent conditions.

Results and discussion

The fluorescence emission wavelength and intensity of an ODN-fluorophore conjugate are not only dependent on the intrinsic properties of the fluorophore but also on its different interactions with the environment including the ODN itself to which it is linked, the complex formed between the ODN–fluorophore conjugate and its target sequence and the solvents. We thought that the linking of a fluorescent label, possessing intercalating properties at the end of ODN probes should place it, upon hybridization of these probes, with either the complementary or the mutated targets in different environments, thus leading to differences in the fluorescent signal emission. We chose thiazole orange (TO) as label for two reasons. First, it fluoresces upon intercalation between the base-pairs of the duplex structures because of the rigidification of the monomethine bridge connecting the two heterocyclics.[29–32] Secondly, unlike many fluorophores, its fluorescence is not greatly quenched by the proximity of guanine.[30,8] End-labelled peptide nucleic acids (PNA–TO conjugates) have been used in real-time PCR analysis[33–35] and phosphodiester oligo-α-thymidylate–TO conjugates were used to detect RNAs inside living cells *via* hybridization with their poly(A) sequences.[36–37] During the course of this work, PNA–TO conjugates involving TO as a base surrogate at the internal position of PNA were reported to discriminate adjacent mismatches.[23] The best discrimination was obtained with T facing TO. In these probes TO is linked *via* a short linker, attached to the quinolinium ring,

Centre de Biophysique Moléculaire CNRS. UPR 4301, affiliated with the University of Orléans and with INSERM, Rue Charles Sadron, 45071, Orléans Cedex 02, France. E-mail: asseline@cnrs-orleans.fr; Fax: +33-2-38-63-15-17

† Electronic supplementary information (ESI) available: Fluorescence data. See DOI: 10.1039/b602262f

forcing it to intercalate. We now report, to our knowledge, the first example of fluorescence detection of terminal mismatches in non stringent conditions. Our strategy is based on the use of sets of oligo-2′-deoxyribonucleotide (ODN) probes linked, *via* their 5′-ends and varying-sized flexible polymethylene chains, to TO with the linker being attached to the benzothiazole moiety (TO′). On the basis of literature results indicating that most intercalators efficiently stabilize duplex structures when linked to ODNs by linkers of a size corresponding to at least 5–6 methylene groups,[38,39] we used a set of linkers with sizes ranging from 4 to 7 methylenes to attach TO′ to the 5′-ends of the ODNs. The sequence of each set of TO′-labelled ODNs was identical and complementary to the sequence to be analyzed on the single-stranded nucleic acid target, except at the interrogation position located at the 5′-end of the probes in position adjacent to the attachment site of TO′, where each of the four nucleic bases were incorporated. As a model for our study, 10-mer-TO′ labelled ODNs and 16-mer ODN targets were chosen so that, upon hybridization, three nucleotides would overhang on each side of the duplexes in order to stabilize them (Fig. 1).[40,41] Furthermore, using this model it is possible to test the influence of the bases present on the target sequence in the position adjacent to the duplex, on the side of the attachment position of TO′ mimicking the interaction of the TO′-labelled ODNs with larger target sequences.

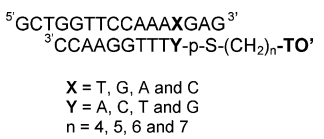

Fig. 1 Structures of the ODN–TO′ conjugates and target sequences.

Since our previous work showed that TO cannot withstand basic deprotection conditions required for the deprotection of an ODN involving the four nucleic bases,[36] we chose to link the TO′ to the ODNs by a reaction between a halogenoalkyl group present on the TO′-linker derivatives and a thiophosphate group incorporated at the 5′-end of ODNs (Fig. 2).

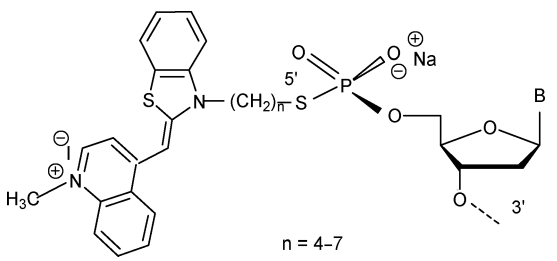

Fig. 2 Structures of the linkage used to connect thiazole orange (TO′) to ODNs in the conjugates.

Synthesis

Synthesis of the TO′-linker derivatives (Scheme 1). The synthesis of the *N*-(ω-halogenoalkyl)-TO′ involving a polymethylene chain in sizes varying from 4 to 7 carbon atoms **6a**–**d** was performed *via* a two-step procedure adapted from the literature[42–44] (Scheme 1). First, the linkers **2a**–**d** were reacted separately with 2-methylbenzothiazole **1** to give the benzothiazole-linker derivatives **3a**–**d**. The latter (1 eq) were then reacted with *N*-methylquinolinium iodide **5**, obtained by reaction of quinoline **4** with methyliodide,[44,45] in CH_2Cl_2, in the presence of NEt_3, to give the TO′-linker derivatives **6a**–**d**.

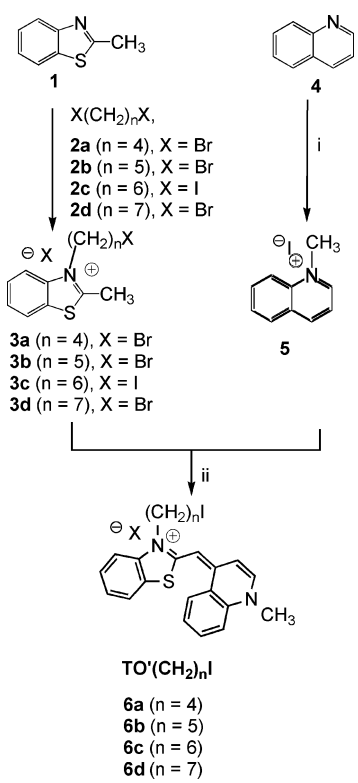

Scheme 1 Synthesis of TO′-linker derivatives **6a**–**d** Reagents and conditions: (i): ICH_3, dioxane; (ii): NEt_3, CH_2Cl_2/MeOH, (50 : 50, *v*/*v*), 1 h, rt.

Synthesis of the ODN–TO′ conjugates (scheme 2). The incorporation of a thiophosphate group at the 5′-terminal position of the ODN bound to the support was performed using our previously reported methods.[46,47] Briefly, after the ODN chain assembly an additional detritylation step was performed to release the 5′-terminal hydroxyl function of the ODNs bound to supports **7**–**10**. The protected thiophosphate group was incorporated at the 5′-end of the ODNs by reaction of a phosphitylating reagent followed by a sulfuration step. After the deprotection step, each of the crude 5′-thiophosphorylated ODNs **11**–**14** was reacted with the four TO′-linker derivatives **6a**–**d** in methanol in the presence of crown ether to give the ODN–TO′ conjugates **15a** to **18d** (see Fig. 2 and Table 1 for the structures). The coupling yields were 50–70%. The Fig. 3 shows the reverse-phase chromatography analysis of the coupling reaction between ODN **12** and the cyanine-linker derivative **6b**. After purification by reverse-phase chromatography, ODN–TO′ conjugates were characterized by electrospray mass spectrometry (Table 1) and UV-visible analysis (Fig. 4). The molar extinction coefficient values (ε) for one conjugate inside each series (ODNs **15d**, **16b**, **17b** and **18d**) were determined by titration of their solutions with the complementary DNA targets as previously reported.[44] The same ε values were used for the conjugates involving the same sequence and different linker lengths to connect the label and the ODNs (Table 1).

Table 1 Characterizations of conjugates

	ODN–TO′ conjugates	Mass analysis		
		Calculated	Found	ε_{260}/M^{-1} cm^{-1}
15a	$^{3'}$CCAAGGTTTA$^{5'}$-*p*-S–$(CH_2)_4$–**TO′**	3468.58	3467.46	—
15b	$^{3'}$CCAAGGTTTA$^{5'}$-*p*-S–$(CH_2)_5$–**TO′**	3482.60	3482.40	—
15c	$^{3'}$CCAAGGTTTA$^{5'}$-*p*-S–$(CH_2)_6$–**TO′**	3496.66	3495.66	—
15d	$^{3'}$CCAAGGTTTA$^{5'}$-*p*-S–$(CH_2)_7$–**TO′**	3510.66	3507.73	121 500
16a	$^{3'}$CCAAGGTTTC$^{5'}$-*p*-S–$(CH_2)_4$–**TO′**	3444.55	3443.34	—
16b	$^{3'}$CCAAGGTTTC$^{5'}$-*p*-S–$(CH_2)_5$–**TO′**	3458.58	3456.06	121500
16c	$^{3'}$CCAAGGTTTC$^{5'}$-*p*-S–$(CH_2)_6$–**TO′**	3472.62	3471.75	—
16d	$^{3'}$CCAAGGTTTC$^{5'}$-*p*-S–$(CH_2)_7$–**TO′**	3486.62	3485.40	—
17a	$^{3'}$CCAAGGTTTT$^{5'}$-*p*-S–$(CH_2)_4$–**TO′**	3459.56	3458.34	—
17b	$^{3'}$CCAAGGTTTT$^{5'}$-*p*-S–$(CH_2)_5$–**TO′**	3473.58	3471.51	119 900
17c	$^{3'}$CCAAGGTTTT$^{5'}$-*p*-S–$(CH_2)_6$–**TO′**	3487.64	3486.00	—
17d	$^{3'}$CCAAGGTTTT$^{5'}$-*p*-S–$(CH_2)_7$–**TO′**	3501.64	3502.80	—
18a	$^{3'}$CCAAGGTTTG$^{5'}$-*p*-S–$(CH_2)_4$–**TO′**	3484.58	3483.72	—
18b	$^{3'}$CCAAGGTTTG$^{5'}$-*p*-S–$(CH_2)_5$–**TO′**	3498.60	3498.00	—
18c	$^{3'}$CCAAGGTTTG$^{5'}$-*p*-S–$(CH_2)_6$–**TO′**	3512.62	3511.56	—
18d	$^{3'}$CCAAGGTTTG$^{5'}$-*p*-S–$(CH_2)_7$–**TO′**	3526.66	3524.97	118 900
27	$^{3'}$TCTCTGGTAA$^{5'}$-*p*-S–$(CH_2)_7$–**TO′**	3500.22	3499.43	133 100
28	$^{3'}$TCTCTGGTAC$^{5'}$-*p*-S–$(CH_2)_7$–**TO′**	3476.19	3474.97	130 900
29	$^{3'}$CTTAGAAAAA$^{5'}$-*p*-S–$(CH_2)_7$–**TO′**	3527.70	3526.10	118 300
30	$^{3'}$CTTAGAAAAC$^{5'}$-*p*-S–$(CH_2)_5$–**TO′**	3543.69	3542.09	112 100

Mass spectrometry analysis and molar absorption coefficients for ODN–TO′ conjugates **15a**–**18d** and **27**–**30**. ε values were determined experimentally for conjugates **15d**, **16b**, **17b** and **18d**.[44] The same ε values were used for the conjugates involving the same sequence and different linker lengths to connect the label and the ODN. For conjugates **27**–**30**, the ε values at $\lambda = 260$ nm were the approximate sum of the ε values of the ODNs[48] and TO′ deducted from that of conjugate **15d** or **16b**.

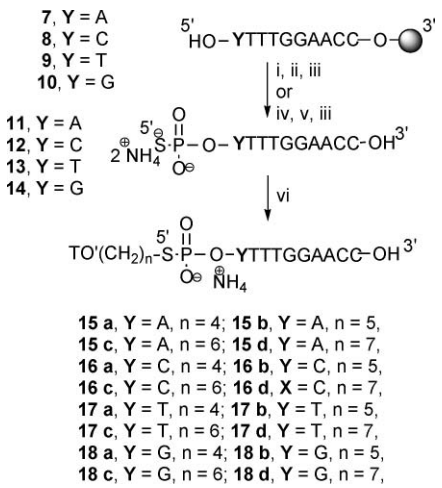

15 a, Y = A, n = 4; **15 b**, Y = A, n = 5,
15 c, Y = A, n = 6; **15 d**, Y = A, n = 7,
16 a, Y = C, n = 4; **16 b**, Y = C, n = 5,
16 c, Y = C, n = 6; **16 d**, X = C, n = 7,
17 a, Y = T, n = 4; **17 b**, Y = T, n = 5,
17 c, Y = T, n = 6; **17 d**, Y = T, n = 7,
18 a, Y = G, n = 4; **18 b**, Y = G, n = 5,
18 c, Y = G, n = 6; **18 d**, Y = G, n = 7,

Scheme 2 Synthesis of ODN–TO′ conjugates **15a** to **18d** Reagents and conditions: (i): $DMTrOCH_2CH_2SSCH_2CH_2$–O–P(O)(H)(O^-) $HNEt_3^+$, pivaloyl chloride; (ii): S_8,CS_2/C_5H_5N; (iii): NH_4OH, overnight, 55 °C; (iv): bis-(2-cyanoethyl)-diisopropylamidophosphite, tetrazole; (v): 3*H*-1,2-benzodithiol-3-one-1,1-dioxide (Beaucage reagent); (vi): TO′$(CH_2)_n$I (among **6a**–**6d**), 18-crown-6 in MeOH, 6 h at rt.

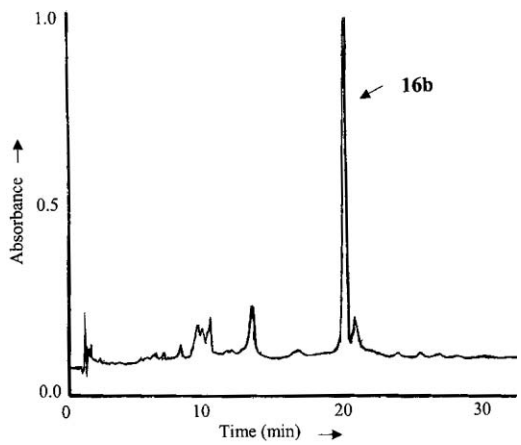

Fig. 3 Reversed-phase HPLC analysis of the coupling reaction between ODN **12** and the cyanine-linker derivative **6b** performed on a Lichrospher RP 18 (5 μm) column (125 × 4 mm) from Merck using a linear gradient of CH_3CN (0 to 35% over 35 min) in 0.1 M aqueous TEAA, pH = 7, with a flow rate of 1 cm^3 min^{-1}. Detection $\lambda = 260$ nm.

Hybridization studies

Linker length selection. Fluorescence studies were conducted on each series of conjugates **15a**–**d**, **16a**–**d**, **17a**–**d**, and **18a**–**d** and a set of four target sequences **23**–**26** in different hybridization conditions (See Table 2 and the Experimental section).

The fluorescence intensities of the mismatched duplexes were greater than those of the corresponding matched duplexes and depended on the linker lengths used to connect the ODNs and TO′. The greatest differences, at both room temperature and 6 °C, were obtained with a seven methylene linker when the 5′-terminal nucleic bases on the ODN probes were purines, and with a five methylene linker when they were pyrimidines. The 7-methylene length linker could also be used for the $^{5'}$C-terminal labelled probe (data not shown). The emission spectra of the four selected labelled ODN probes, either free or in the presence of each of the four ODN targets, are shown in Fig. 5 and the discrimination factors listed in Table 2. The discrimination factors were determined as the fluorescence intensity ratio between the mismatched duplexes and the perfectly matched ones (I_{FMM}/I_{FPM}). The greatest discrimination factors between the perfectly matched duplexes and the mismatched ones were obtained when TO′ was

Table 2 T_m values and fluorescence data

	$^{3'}$CCAAGGTTTY$^{5'}$-R		$^{5'}$GCTGGTTCCAAAXGAG$^{3'}$ (targets)											
			23 (X = T)			**24** (X = G)			**25** (X = A)			**26** (X = C)		
	Y	R	T_m [a]	ΔT_m	I_{FMM}/I_{FPM} [b]	T_m [a]	ΔT_m	I_{FMM}/I_{FPM} [b]	T_m [a]	ΔT_m	I_{FMM}/I_{FPM} [b]	T_m [a]	ΔT_m	I_{FMM}/I_{FPM} [b]
15d	A	–*p*-$(CH_2)_7$TO′	**36**	—	—	20	16	4.16	24	12	6.25	27	9	5.1
19	A	–H	**27**	—	—	16	11	—	19	8	—	19	8	—
16b	C	–*p*-$(CH_2)_5$TO′	23	5	3.14	**28**	—	—	24	4	2.30	23	5	2.80
20	C	–H	19	3	—	**22**	—	—	18	4	—	15	8	—
17b	T	–*p*-$(CH_2)_5$TO′	25	3	3.3	20	8	5.30	**28**	—	—	25	3	6.60
21	T	–H	20	2.5	—	15.5	7	—	**22.5**	—	—	21	1.5	—
18d	G	–*p*-$(CH_2)_7$TO′	28	11	2.3	19	18	2.85	19	18	4.5	**37**	—	—
22	G	–H	22.5	5	—	23	4.5	—	21	6.5	—	**27.5**	—	—

[a] Duplex concentrations were $[C] = 1$ μM (each strand) in a 5 mM sodium cacodylate buffer, pH = 6, containing 50 mM NaCl. T_m values are given in °C. Errors in T_ms are estimated as ±1 °C. ΔT_m values (in °C) correspond to the T_m difference between those of the perfectly matched duplexes and the mismatched ones. [b] I_{FMM}/I_{FPM} = discrimination factor. Fluorescence intensities were measured at $\lambda = 530$ nm for the mismatched duplexes and the corresponding perfectly matched ones hybridized at 6 °C. Duplex concentrations and buffer conditions were the same as for T_m measurements.

Fig. 4 UV-visible absorption spectrum of conjugate **18d** recorded between $\lambda = 230$ and $\lambda = 580$ nm in a 5 mM sodium cacodylate, pH = 7, buffer containing 50 mM NaCl.

Fig. 5 Fluorescence emission spectra of the conjugates $^{3'}$CCAAGGTTTY-*p*-S–$(CH_2)_n$-TO′, [**15d**: Y = A, $n = 7$ (A); **16b**: Y = C, $n = 5$ (B); **17b**: Y = T, $n = 5$ (C) and **18d**: Y = G, $n = 7$ (D)] free (plain), hybridized with $^{5'}$GCTGGTTCCAAAXGAG$^{3'}$: **23**, X = T(◇); **24**, X = G (□); **25**, X = A (△); and **26**, X = C (+) (calibration based on fluorescence of free probes) recorded at 6 °C in a 5 mM sodium cacodylate, pH = 6, buffer containing 50 mM NaCl, after 30 min incubation. [conjugate] = [target] = 1 μM. $\lambda_{exc} = 465$ nm.[34]

linked in the position adjacent to A (discrimination factor >4) and to T (discrimination factor >3). When TO′ was attached close to C or G the discrimination factor remained at least superior to 2.3. In addition, the λ_{max} emission of the matched duplexes were slightly red-shifted as compared to those of the mismatched ones (3–4 nm when the TO′ was linked close to the purine bases, 2–3 nm when it was close to C and only 1 nm when in the proximity of *T*). These new probes are clearly able to discriminate mismatches ones such as G/A, A/G, T/T, C/C, C/T or T/C, reportedly difficult to distinguish from the corresponding perfect base-pairs by the cellular repair machinery.[49] It should be noted that the detection of mismatched base-pair located at internal position of duplexes with PNA probes involving TO as base surrogate was efficiently achieved only when TO was attached to the probes *via* the lepidinium nucleus.[23] In the TMDFO reported here TO was

linked *via* the benzothiazole nuclei. ODN probes in which TO was attached through the lepidine were not efficient at discriminating the four perfect base-pair from their corresponding mismatched ones (data not shown). Furthermore, when using TMDFOs the mismatched duplexes are more fluorescent than the perfectly matched ones in opposition to the results obtained with the PNA–TO conjugates[22,23] and most of the other ODN–fluorophore conjugates designed to detect mismatches at internal positions of duplexes.[12–14,16–18,20–21]

In order to gain information on the stability of the different series of fully matched and mismatched duplexes, the T_m values for the sixteen duplexes formed between the four selected ODN–TO′ conjugates **15d**, **16b**, **17b** and **18d** and each target sequence **23**–**26** were determined using the same concentrations and buffer conditions as those used for the fluorescence experiments and then compared to the corresponding unlabelled duplexes (Table 2). Different results were obtained. First, it was confirmed that for the same base-pair composition, the T_m values for the perfect duplexes depended on the sequence context.[25,50] Consequently, in many cases the T_m values for the matched and mismatched duplexes were not very different. Secondly, the presence of TO′ stabilized all the duplexes except those containing GG or GA mismatches, as the label was attached close to G (**18d** + **24** and **18d** + **25**) and the visible λ_{max} absorption was slightly red-shifted (1– 2 nm) for the perfect duplex compared to that of the mismatched ones (except when TO′ was linked in a position adjacent to C for which no difference was noted). Thirdly, in most cases, the ΔT_m difference between the mismatched and perfectly matched duplexes was strongly increased by the presence of TO′ attached close to the purine bases and slightly increased or not at all when it was attached close to the pyrimidine bases (Table 2). Only in one case, when a C/C mismatch was present at the end of the duplex (**16b** + **26** and **20** + **26**) the ΔT_m difference between the mismatched and perfectly matched duplexes was slightly reduced by the presence of the TO′. These results clearly indicated the absence of a correlation between the ΔT_m observed for the matched and mismatched duplexes and their emission intensity ratio. Considering the fact that all the duplexes, labelled and unlabelled, possess the same number of negative charges and that mismatches are reportedly generally stacked in a B-type right-handed helix but undergo greater dynamical motion than the perfectly matched base-pairs,[51–53] it is likely that the different stabilizations induced by the presence of TO′ are due to its different interactions with the ends of the duplexes. The important emission enhancement of thiazole orange, upon its interaction with double-stranded duplexes, is acknowledged as being the result of the induced restriction of torsion around the central methine bridge.[30] It has also been suggested that the emission quenching by electron transfer was not a very important process.[30] In the presence of mismatched base-pairs, the stability, if any, induced by the presence of TO′ was weaker than for the perfectly matched duplexes. The greater fluorescence emission observed in these cases is consistent with a reduced rate of fluorescence quenching, through a charge transfer between the nucleic base-pairs and the label, because of the looser contacts between TO′ and the duplexes and of the presence of loosely paired bases due to the loss of hydrogen-bonding.[53,54] The strong differences observed for the fluorescence emission of the matched and mismatched duplex may also be due to the different expositions of TO′ to the solvents. Further studies are needed to determine the structures of the matched and mismatched duplexes.

Influence of the nucleic base neighboring on the mismatch detection. In order to test the viability of our system, we have also tested the influence of the presence of mismatches at the penultimate position of the duplexes by performing the hybridizations of the four ODN–TO′ conjugates **15d**, **16b**, **17b** and **18d** with 16 target sequences (Fig. 6). The targets were ODNs **23**–**26** involving Z = A and those with Z = T, G or C. The results of the fluorescence studies indicated that the TMDFOs are not only able to discriminate perfect duplexes from those involving a terminal mismatch, but also from those involving mismatches at the penultimate or last two positions (refer to the ESI for fluorescence data).

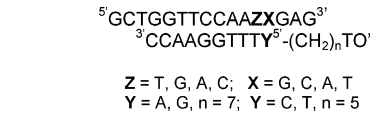

Fig. 6 Sequences used to study the influence of mismatches at the penultimate and last two positions of the duplexes.

To further test the viability of our system, the influence of the nucleic base V present on the dangling end in the position adjacent to the duplexes on the side of the TO′ attachment was also studied (Fig. 7, and the ESI for fluorescence data).

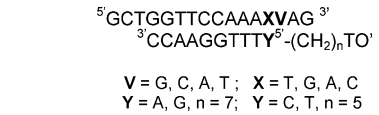

Fig. 7 Sequences used to study the influence of the nucleic bases present on the target sequence in the position adjacent to the duplex.

The results indicated that the discrimination between the matched and mismatched duplexes was also possible when G (V = G) was replaced by A or T, (V = A or T) or reduced when two consecutive C were present on the target sequence [the one involved in the terminal base-pair (X = C) of the duplexes and the other on the dangling end (V = C)].

Influence of the sequence context on the terminal mismatch detection. The model reported above corresponds to mutations of T into G or A at position 3434 (exon 17b) of the CFTR gene.[55,56] In order to study the influence of the sequence, we applied our hybridization format to the analysis of the G/T mutation present at position 135 (exon 1) and T/G mutation at position 395 (exon 3) (Fig. 8). The ODN–TO′ conjugates **27** and **28** required for the position 135 analysis and ODN–TO′ conjugates **29** and **30** for the position 395 analysis were prepared as reported above for the synthesis of conjugates **15a** to **18d** (see Table 1 for characterizations). A seven methylene linker was used for the attachment of TO′ close to a 5′-terminal purine base (**27** and **29**) while for its attachment in the vicinity of a pyrimidine base either a seven methylene linker (ODN **28**) or a five methylene linker (ODN **30**) were employed (in accordance with the results obtained with our model system (*vide supra*)). Discrimination factors superior to 2 and 3 were obtained, respectively.

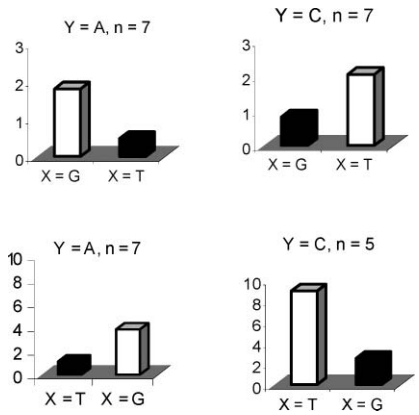

Fig. 8 Fluorescence duplex/fluorescence free probes for matched (black bars) and mismatched (white bars) at room temperature. Duplexes formed between conjugates $^{3'}$TCTCTGGTAY$^{5'}$–$(CH_2)_n$TO′ **27** (Y = A, n = 7) and **28** (Y = C, n = 7) and the target sequences $^{5'}$CCGAGAGACCATXCAG$^{3'}$ (X = G, T) (top) and duplexes formed between conjugates $^{3'}$CTTAGAAAAY$^{5'}$–$(CH_2)_n$TO′: **29** (Y = A, n = 7), **30** (Y = C, n = 5) and the target sequences $^{5'}$ATGGAATCTTTTXATA$^{3'}$ (X = T, G) (low). Concentrations and buffers were the same as for Fig. 5.

Conclusions

We have reported new fluorescent ODN probes for the detection of mismatches located at the ends of the DNA duplexes in non-stringent conditions. This method is based on the use of a set of DNA probes, labelled at their 5′-ends with a thiazole orange TO′ *via* linkers of varying sizes attached to the benzothiazole ring (TO′), and two fluorescent measurements at the same temperature, one for the free probes and the second after addition of the target single-stranded nucleic acid sequences to be analyzed. These ODN–TO′ conjugates are not only able to discriminate perfect duplexes from those involving a terminal mismatch, but also from those involving mismatches at the penultimate or last two positions. Contrary to what was observed with the majority of the previously reported fluorescent ODN probes, capable of detecting the presence of mismatches when located at the internal positions of the duplexes, the mismatched duplexes were more fluorescent than the perfect ones (at least more than two-fold) using our new terminal mismatch discriminating fluorescent oligonucleotides (TMDFO). Our system was successfully applied to the analysis of a few mutations of the CFTR gene used as models. These new probes are inexpensive and stable in water or buffer solutions over a long period of time (more than two years) at −20 °C. They are promising tools for the detection of terminal mismatched base-pairs in high throughput based hybridization analyses including sequencing and provide a new hybridization scheme for the analysis of mutations. Future work will be aimed at testing their performance in other sequence contexts and studying the structure of the matched and mismatched duplexes.

Experimental

Materials and methods

All solvents used were of the highest purity and did not contain more than 10 ppm H_2O. All chemicals were used as obtained unless otherwise stated. 2-Methylbenzothiazole, methyliodide, quinoline, 1,4-dibromobutane, 1,5-dibromopentane, 1,6-diiodohexane, 1,7-dibromoheptane, acetic anhydride, DTT and dioxane were purchased from Aldrich. Triethylamine and sodium sulfate were purchased from Merck, pyridine and dichloromethane from SDS, acetonitrile, methanol from Labo-Standa. Analytical thin-layer chromatography (TLC) was performed on precoated alumina plates (Merck silica gel 60F 254 ref. 5554). During all the synthesis and purification steps, thiazole orange derivatives were protected from light. Preparative TLC was performed on glass-backed plates (Merck silica gel 60F 254 ref. 5717). For flash chromatography, Merck silica gel 60 (70–230 mesh) (ref. 7734) was used. Compounds were directly visualized on the plates as colored spots. ODNs were synthesized using cyanoethyl phosphoramidite chemistry and an expedite nucleic acid synthesis system 8909 from PerSeptive Biosystems. Reverse-phase chromatography analysis was performed on a 600 E (System Controller) equipped with a photodiode array detector Waters 990 using a Lichrospher 100 RP 18 (5 μm) column (125 mm × 4 mm) from Merck with a linear gradient of CH_3CN in 0.1 M aqueous triethylammonium acetate, pH 7, with a flow rate of 1 cm^3 min^{-1}. ^{1}H-NMR and ^{13}C-NMR spectra were recorded on a Varian Unity 500 Spectrometer. ^{1}H Chemical shifts were referenced to either a residual solvent peak DMSO (2.54 ppm) or Me_4Si. ^{1}H NMR coupling constants are reported in Hz and refer to apparent multiplicities. Mass analysis ion-molecular weights of the ODNs were confirmed by electrospray mass spectroscopy using a Quattro II (MicroMass) instrument. Absorption spectra were recorded with a Uvikon 860 spectrophotometer (spectral band width 1 nm). Steady-state fluorescence experiments were performed on a Fluoromax 2 (ISA-Jobin-Yvon) spectrofluorimeter in 0.5 cm path-length Suprasil quartz cuvettes (Hellma) with slits set at 0.5 mm (band pass = 2 nm) and on a Cytofluor II fluorescence multi-well plate reader (Biosearch). The spectra were corrected for the different output of the excitation lamp at the different wavelengths used for the experiment. In order to avoid inner filter effects and light re-absorption, solutions with maximal absorbance at the excitation wavelength below 0.1 were used.

Synthesis of the thiazole orange analogue-linker derivatives TO′$(CH_2)_n$X

General procedure for the preparation of the benzothiazolinium-linker derivatives **3a**–**d** (n = **4**–**7**)

A mixture of 2-methylbenzothiazole **1** (1 eq, 1 mmol) and bis-halogenoalkyl linkers **2a**–**d** (1,4-dibromobutane; 1,5-dibromopentane; 1,6-diiodohexane or 1,7-dibromoheptane) (5 eq, 5 mmol) was heated for 3 h at 140 °C to give a dark brown colored solution. After cooling to room temperature, the reaction mixture was washed with pentane and then purified on a silica gel column using a MeOH gradient (0 to 8%) in CH_2Cl_2 to give grey solids. **3a** (200 mg, n = 4, 54%), **3b** (150 mg, n = 5, 40%), **3c** (121 mg, n = 6, 25%) and **3d** (81 mg, n = 7, 20%).

***N*-(4-Bromobutyl)-2-methylbenzothiazolium bromide (3a).** ^{1}H NMR (500 MHz, $CDCl_3$, TMS): δ = 8.23–8.19 (2H, m, H_{Ar}), 7.90–7.85 (1H,m, H_{Ar}), 7.76 (1H, t, 7.7 Hz, H_{Ar}) 5.11 (2H, t, J = 8.2 Hz, N^+CH_2), 3.61–3.57 (5H, m, CH_3 +CH_2Br), 2.23–2.17 (4H, m, $2CH_2$). ESI-MS: m/z, $C_{12}H_{15}BrNS$, calcd 284.01 and 286.0, found 285.71 and 287.73 (M^+).

***N*-(5-Bromopentyl)-2-methylbenzothiazolium bromide (3b).** ^{1}H NMR (500 MHz, $CDCl_3$, TMS): δ = 8.24 (1H, d, J = 8.14 Hz, H_{Ar}), 8.07 (1H, d, J = 8.56 Hz, H_{Ar}), 7.89–7.84 (1H, m, H_{Ar}), 7.78–7.74 (1H, m, H_{Ar}), 5.03 (2H, t, J = 7.9 Hz, N^+CH_2), 3.56 (3H, S, CH_3), 3.44 (2H, t, J = 6.4 Hz, CH_2Br), 2.10–2.02 (2H, m, CH_2), 2.02–1.95 (2H, m, $2CH_2$), 1.77–1.69 (2H, m, CH_2). ESI-MS: m/z, $C_{13}H_{17}BrNS$ calcd 299.02. and 301.01, found 298.95 and 301.10 (M^+).

***N*-(6-Iodohexyl)-2-methylbenzothiazolium iodide (3c).** ^{1}H NMR (500 MHz, $CDCl_3$, TMS): δ = 8.32 (1H, d, J = 9.0 Hz, H_{Ar}), 8.09 (1H, d, J = 8.6 Hz, H_{Ar}), 7.85 (1H, t, J = 7.9 Hz, H_{Ar}), 7.74 (1H, t, J = 7.75 Hz, H_{Ar}), 4.90 (2H, t, J = 9.9 Hz, N^+CH_2), 3.49 (3H, S, CH_3), 3.19 (2H, t, J = 7.8 Hz, CH_2I), 2.04–1.96 (2H, m, CH_2), 1.87–1.79 (2H, m, CH_2), 1.60–1.48 (4H, m, 2 CH_2). ESI-MS: m/z, $C_{14}H_{19}IN_2S$ calcd 360.02, found 360.06 (M^+).

***N*-(7-Bromoheptyl)-2-methylbenzothiazolium bromide (3d).** ^{1}H NMR (500 MHz, $CDCl_3$, TMS): δ = 8.33 (1H, d, J = 7.8 Hz, H_{Ar}), 8.03 (1H, d, J = 7.7 Hz, H_{Ar}), 7.85–7.79 (1H, m, H_{Ar}), 7.74–7.68 (1H, m, H_{Ar}), 5.02–4.88 (2H, m, N^+CH_2), 3.53 (3H, S, CH_3), 3.41 (2H, t, J = 6.4 Hz, CH_2Br), 2.02–1.94 (2H, m, CH_2), 1.89–1.83 (2H, m, CH_2), 1.54–1.40 (6H, m, 3 CH_2). ESI-MS: m/z, $C_{15}H_{21}BrNS$ calcd 326.05 and 328.05, found 326.11 and 328.10 (M^+).

***N*-Methylquinolinium iodide (5).** A mixture of quinoline (525 mg, 4 mmol, 1eq), iodomethane (2.84 g, 20 mmol, 5 eq and dioxane (10 cm^3) was heated at 80 °C in a sealed flask for 2 h. The mixture was allowed to cool to room temperature, the solid was collected by filtration, washed with Et_2O and dried under vacuum to give an orange solid (940 mg, 85%). ^{1}H NMR (500 MHz, $CDCl_3$, TMS): δ = 10.48 (1H, d, J = 5.68 Hz, H_{Ar}), 8.98 (1H, d, J = 8.42 Hz, H_{Ar}), 8.36 (1H, d, J = 8.85 Hz, H_{Ar}), 8.31–8.24 (2H, m, H_{Ar}), 8.19–8.14 (1H, m, H_{Ar}), 8.06–8.01 (m, 1H, H_{Ar}), 3.71 (3H, s, CH_3). ESI-MS: m/z, $C_{10}H_{10}N^+$ calcd 144.08, found 142.91 (M^+).

General procedure for the preparation of the thiazole orange-linker derivatives 6a–d (n = 4–7). A mixture of the methylbenzothiazole linker derivatives **3a–d** (n = 4, 5, 6 or 7) (1 eq), *N*-methylquinolinium iodide **5** (1 eq), dry CH_2Cl_2–MeOH (50 : 50, v/v) and NEt_3 (2.5 eq) was stirred, for 3 h at rt to give a red colored solution. After removal of the solvent by evaporation, the residue was purified on a silica gel column using a MeOH gradient (0 to 4%) in CH_2Cl_2) then on preparative silica gel plates using a CH_2Cl_2–MeOH–acetone mixture (165 : 6 : 18, $v/v/v$) as eluent to give red solids. Yields: 12–15%. Compounds were analyzed by ^{1}H NMR, ^{13}C-NMR and mass spectrometry. The results of the mass spectrometry analysis are in accordance with halogen exchange during the synthesis that occurs in basic conditions. This phenomenon was already observed in our previous work.[35]

3-(4-Iodobutyl)-4-[(1,4-dihydro-1-methylquinolin-4-ylidene)-methyl]benzothiazolium iodide (6a). ^{1}H NMR (500 MHz, d6-DMSO): δ = 8.82–8.78 (1H, m, H_{Ar}), 8.64 (1H, d, J = 7.2 Hz, H_{Ar}), 8.11–8.01 (3H, m, H_{Ar}), 7.83–7.77 (2H, m, H_{Ar}), 7.64–7.59 (1H, m, H_{Ar}), 7.45–7.40 (2H, m, H_{Ar}), 6. 94 (1H, s, = CH–), 4.67 (2H, t, J = 7.09 Hz, $–CH_2–N^+$), 4.19 (3H, s, N^+CH3), 3.39 (2H, t, J = 6.63 Hz, CH_2–I), 2.08–1.84 (4H, m, 2 CH_2). ^{13}C NMR (500 MHz, DMSO): δ = 159.21, 148.89, 145.14, 139.97, 138.08, 133.27, 128.22, 127.02, 125.61, 124.52, 124.07, 123.84, 122.97, 118.33, 112,92, 108.11, 87.53, 44.57, 42.46, 29.94, 27.82, 8.32). ESI-MS: m/z, $C_{22}H_{22}N_2SI$ calcd 473.05, found 473.14 (M^+).

3-(5-Iodopentyl)-4-[(1,4-dihydro-1-methylquinolin-4-ylidene)-methyl]benzothiazolium iodide (6b). ^{1}H NMR (500 MHz, $CDCl_3$, TMS): δ = 9.07 (1H, d, J = 7.79 Hz, H_{Ar}), 8.63 (1H, d, J = 8.0 Hz, H_{Ar}), 7.83 (1H, t, J = 7.23 Hz H_{Ar}), 7.77 (1H, t, J = 7.29 Hz, H_{Ar}), 7.70 (1H, d, J = 7.7 Hz, H_{Ar}), 7.65 (1H, d, J = 8.45 Hz, H_{Ar}), 7.50 (1H, t, J = 7.79 Hz, H_{Ar}), 7.43 (1H, d, J = 7.16 Hz, H_{Ar}), 7.36–7.28 (2H, m, H_{Ar}), 6. 74 (1H, s, = CH–), 4.54 (2H, t, J = 7.46 Hz, $–CH_2–N^+$), 4.22 (3H, s, N^+CH_3), 3.22 (2H, t, J = 6.75 Hz, CH_2–I), 2.10–1.90 (4H, m, 2 CH_2), 1.78–1.68 (2H, m, CH_2). ^{13}C NMR (500 MHz, $CDCl_3$, TMS): δ = 159.66, 149.40, 145.73, 139.96, 138.19, 133.21, 128.35, 127.60, 126.16, 124.87, 124.68, 124.60, 122.86, 117.05, 112,15, 109.38, 88.05, 47.10, 43.24, 32.85, 28.04, 26.42, 6.63). ESI-MS: m/z, $C_{23}H_{24}N_2SI$ calcd 487.07, found 487.15 (M^+).

3-(6-Iodohexyl)-4-[(1,4-dihydro-1-methylquinolin-4-ylidene)-methyl]benzothiazolium iodide (6c). ^{1}H NMR (500 MHz, $CDCl_3$, TMS): δ = 8.95 (1H, d, J = 7.2 Hz, H_{Ar}), 8.65 (1H, d, J = 8.4 Hz, H_{Ar}), 8.80–7.75 (2H, m, H_{Ar}), 7.69 (1H, d, J = 9.0 Hz, H_{Ar}), 7.59 (1H, t, J = 8.34 Hz, H_{Ar}), 7.47 (1H, t, J = 8.34 Hz, H_{Ar}), 7.34 (1H, t, J = 7.16 Hz, H_{Ar}), 7.31–7.26 (2H, m, H_{Ar}), 6. 73 (1H, s, = CH–), 4.54 (2H, t, J = 8.5 Hz, $CH_2–N^+$), 4.14 (3H, s, N^+CH_3), 3.19 (2H, t, J = 6.8 Hz, CH_2–I), 1.96–1.89 (2H, q, m, CH_2), 1.86–1.79 (2H, m, CH_2), 1.69–1.55 (2H, m, CH_2), 1.54–1.48 (2H, m, CH_2). ^{13}C NMR (500 MHz, $CDCl_3$, TMS): δ = 159.58, 149.14, 145.43, 139.95, 138.06, 133.15, 128.30, 127.62, 126.28, 124.78, 124.68, 124.47, 122.81, 117.00, 112,24, 109.14, 88.23, 47.26, 43.06, 33.15, 30.40, 27.42, 26.08, 7.30). ESI-MS: m/z, $C_{24}H_{26}N_2SI$ calcd 501.08, found 501.15 ($M^{+)}$.

3-(6-Iodoheptyl)-4-[(1,4-dihydro-1-methylquinolin-4-ylidene)-methyl]benzothiazolium iodide (6d). ^{1}H NMR (500 MHz, $CDCl_3$, TMS): δ = 9.0 (1H, d, J = 7.2 Hz, H_{Ar}), 8.61 (1H, d, J = 8.0 Hz, H_{Ar}), 7.82 (1H, t, J = 7.24 Hz, H_{Ar}), 7.75 (1H, t, J = 7.24 Hz, H_{Ar}), 7.69 (1H, d, J = 8.5 Hz, H_{Ar}), 7.62 (1H, d, J = 8.5 Hz, H_{Ar}), 7.49 (1H, t, J = 7.32 Hz, H_{Ar}), 7.38 (1H, d, J = 7.17 Hz, H_{Ar}), 7.32–7.28 (2H, m, H_{Ar}), 6. 73 (1H, s, = CH–), 4.63 (2H, t, J = 6.9 Hz, $CH_2–N^+$), 4.18 (3H, s, N^+CH_3), 3.15 (2H, t, J = 8.4 Hz, CH_2–I), 1.95–1.88 (2H, m, CH_2), 1. 83–1.77 (2H, m, CH_2), 1.58–1.54 (2H, m, CH_2), 1.45–1.35 (4H, m, 2 CH_2). ^{13}C NMR (500 MHz, $CDCl_3$, TMS): δ = 159.67, 149.22, 145.55, 140.02, 138.15, 133.17, 128.29, 127.52, 126.10, 124.80, 124.72, 124.53, 122.83, 117.08, 112.22, 109.22 88.16, 47.35, 43.06, 33.38, 30.31, 28.46, 27.48, 26.98, 7.32). ESI-MS: m/z, $C_{25}H_{28}N_2SI$ calcd 515.10 found 515.17 (M^+).

Synthesis of the 5′-thiophosphorylated ODNs 7–10

The ODNs were assembled using conventional phosphoramidite methodology with an Expedite 8909 DNA synthesizer at the one micromole scale. At the end of the chain assembly an additional detritylation step was performed. At this step the incorporation of the thiophosphate group can be performed following two strategies.

Strategy A. The H-phosphonate derivative $DMTOCH_2$-$CH_2SSCH_2CH_2OP(O)(H)(O^-)$ $HNEt_3^+$ (0.025 g, 0.04 mmol) [in a pyridine–CH_3CN mixture (50 : 50, v/v) (0.4 cm^3) dried

overnight on 3 Å molecular sieves] and pivaloyl chloride (0.020 g, 0.166 mmol) in CH_3CN solution (0.5 cm^3) [prepared one hour before use and dried over 3 Å molecular sieves] were added simultaneously. After a 2.5 min of reaction the solution was removed and the support washed three times with 1 cm^3 of an anhydrous pyridine–CH_3CN mixture (50 : 50, *v*/*v*). The sulfurization step was performed by addition of a sulfur solution [50 mg S_8 in a CS_2–pyridine mixture (3 : 2 *v*/*v*), 2 cm^3]. After 20 min of reaction the solution was removed and the support was washed three times with a pyridine–CH_3CN mixture and then with 1 cm^3 acetonitrile (three times). After the deprotection step and releasing from the support by an overnight treatment with concentrated aqueous ammonia at 55 °C containing DTT (50 eq), the ammonia was removed under vacuum.

Strategy B. 0.2 M solution of bis-(2-cyanoethyl)diisopropyl-amidophosphite in CH_3CN (0.2 cm^3) and 0.5 M solution of tetrazole in CH_3CN (0.5 cm^3) were added simultaneously to the ODNs bound to the support. After 10 min reaction the solution was removed. A 0.5 M solution of 3*H*-1,2-benzodithiole-3-one-1,1-dioxide (Beaucage reagent)[57] in CH_3CN (1 cm^3) was added. After 10 min reaction the solution was removed and the support washed with 1 cm^3 CH_3CN (three times). After the deprotection step and releasing from the support by an overnight treatment with concentrated aqueous ammonia at 55 °C containing DTT (50 eq), the ammonia was removed under vacuum.

The crude ODN solution was then concentrated to a volume of 1.5 cm^3 and loaded on a G25 Sephadex column. Samples of 10 OD of crude 5′-thiophosphorylated ODNs were lyophilized separately.

ODN labelling

To vortexed solutions of ODNs 5′-thiophosphorylated (10 OD each) in MeOH (0.4 cm^3) containing 18-crown-6 ether (10 mg) were added methanolic solutions of the TO′-linker derivatives **6** (1.5 mg in 0.4 cm^3). After a 17 h reaction, the coupling efficiency was controlled by reverse-phase chromatography with a linear gradient of CH_3CN (5 to 50% over 60 min) in 0.1 M aqueous triethylammonium acetate, pH 7, with a flow rate of 1 cm^3 min^{-1}. Retention times increased with the size of the chain used to connect TO′ and the ODNs. The crude mixture was evaporated to dryness, and solubilized with a 1 M NaH_2PO_4 solution pH 6 containing 10% MeOH (1 cm^3). The dye excess was extracted with CH_2Cl_2 (3 × 3 cm^3). Aqueous phase was loaded on a Sephadex G25 column and the fast eluting colored fractions were purified using the conditions described above. (See Table 1 for mass analysis data). Coupling yields 60 to 80%.

UV/visible absorption measurements

Molar absorption coefficient determination. The molar absorption coefficients ($\varepsilon_{260\,nm}$ values) for the conjugates **15d**, **16b**, **17b**, and **18d** were determined by titrations of the ODN–TO′ solutions in a 5 mM sodium cacodylate buffer containing 50 mM NaCl, pH 6, performed at 3 °C, with solutions of the single-stranded complementary sequences. Concentrations of ODN targets were calculated using molar extinction coefficients at 260 nm determined using the nearest-neighbor model.[48] The same $\varepsilon_{260\,nm}$ values were used for each series of conjugates involving the same ODN sequence and different linker sizes. For the other conjugates the $\varepsilon_{260\,nm}$ values were estimated to be the sum of the ε values of the ODNs and of the cyanines deducted from the titrations (see Table 1).

***T*$_m$ measurements.** The T_m values for the four matched and the twelve mismatched duplexes formed between the conjugates $^{3'}$CAAGGTTTY-*p*-S–$(CH_2)_n$-TO′ **15d** (Y = A, *n* = 7); **16b** (Y = C, *n* = 5); **17b** (Y = T, *n* = 5); **18d** (Y = G, *n* = 7) and the target sequences $^{5'}$GCTGGTTCCAAAXGAG$^{3'}$ X = T, G, A or C (as well as for the corresponding unlabelled duplexes) were determined by thermal denaturation followed by absorption spectroscopy[44] using 1 μM solutions of duplexes (each strand) in a 5 mM sodium cacodylate buffer, pH 6, containing 50 mM NaCl. Results are given in Table 2. The uncertainty in the T_m values reported was ±1 °C.

Fluorescence experiments

General. Fluorescence excitation and emission spectra were recorded on a Fluoromax 2 (ISA-Jobin-Yvon) spectrofluorimeter in 0.5 cm path-length Suprasil quartz cuvettes (Hellma) with slits set at 0.5 mm (band pass = 2 nm). A 1 μM solution of labelled ODNs was prepared in a 5 mM sodium cacodylate, buffer containing 50 mM sodium chloride, pH 6 (0.6 cm^3). The double-stranded samples were prepared by addition of a small volume (5 μl) of a concentrated solution of the appropriate target sequences (1 eq) at room temperature. The sample was left to hybridize 30 min at 6 °C (far below the T_m value) in the dark before the measurements were performed. Fluorescence emission spectra (with excitation at 465 nm)[33] of free and hybridized probes (involving fully matched and mismatched duplexes) were recorded between λ = 470 and 700 nm. Spectra recorded between λ = 500 and 600 nm are shown in Fig. 5.

Experiments were also performed with a Cytofluor II reader plate [λ_{Ex} 485 nm/λ_{Em} 530 nm] in order to perform parallel reading of several samples. The hybridizations were performed with 1 μM solutions (0.1 cm^3) of the ODN–TO′ probes in a 5 mM cacodylate buffer, pH 7 or 6, containing 50 mM NaCl placed in a 96-well plate. Measurements were performed at either room temperature (25 °C) or after incubation at 6 °C for different times (15, 30, 45 min, and 1 h 30 min). A first fluorescence measurement was performed with solutions of the free probes. Then one equivalent of the target sequences to be analyzed (5 μl of a concentrated solution) were added to the ODN–TO′ solutions and a second fluorescence measurement was performed. A comparison of the fluorescence values obtained for the free ($F_{free\ probe}$) and the hybridized ODN–TO′ probes (F_{duplex}) at the same temperature allowed the detection of the fully matched duplex. In any case, the $F_{duplex}/F_{free\ probe}$ ratio obtained for the perfect duplex was lower than those obtained for the corresponding mismatched duplexes. Errors in fluorescence values are estimated to be ±10%.

Selection of the linker length. The hybridizations of the conjugates **15a** to **18d** involving different linker lengths $^{3'}$CCAAGGTTTY-*p*-S–$(CH_2)_n$-TO′ (Y = A, C, T, G, *n* = 4–7) with the target sequences $^{5'}$GCTGGTTCCAAAXGAG$^{3'}$ (X = T, G, A and C) were performed with a Cytofluor II reader plate using different conditions (*vide supra*). The results indicated the best discrimination factors for the conjugates $^{3'}$CCAAGGTTTY-*p*-S–$(CH_2)_n$-TO′, **15d** (Y = A, *n* = 7), **16b** (Y = C, *n* = 5), **17b**

(Y = T, $n = 5$ or 7), and **18d** (Y = G, $n = 7$) after hybridization at either room temperature or 6 °C (data not shown).

Acknowledgements

We thank the CNRS "Programme Puces à ADN" for financial support, H. Meudal and C. Buré for recording the NMR spectra and for running the electrospray mass spectrometer.

References

1 International Human Genome Sequencing Consortium: *Nature*, 2001, **409**, 860.
2 J. C. Venter, M. D. Adams, E. W. Myers, P. W. Li, R. J. Mural, G. G. Sutton, H. O. Smith, M. Yandell, C. A. Evans and R. A. Holt, *et al.*, *Science*, 2001, **291**, 1304.
3 D. Botstein and N. Risch, *Nat. Genet.*, 2003, **33**, 228.
4 H. C. Erichsen and S. J. Chanock, *Br. J. Cancer*, 2004, **90**, 747.
5 C. S. Carlson, M. A. Eberle, M. J. Rieder, J. D. Smith, L. Kruglyak and D. A. Nickerson, *Nat. Genet.*, 2003, **33**, 518.
6 B. W. Kirk, M. Feinsod, R. Favis, R. M. Kliman and F. Barany, *Nucleic Acids Res.*, 2002, **30**, 3295.
7 A. P. Silverman and E. T. Kool, *Trends Biotechnol.*, 2005, **23**, 225.
8 U. Asseline, *Curr. Org. Chem.*, 2006, **10**, 491.
9 A. Okamoto, K. Tanaika and I. Saito, *J. Am. Chem. Soc.*, 2003, **125**, 4972.
10 A. Okamoto, K. Tanaka, T. Fukuta and I. Saito, *J. Am. Chem. Soc.*, 2003, **125**, 9296.
11 A. Okamoto, K. Tanaika and I. Saito, *Tetrahedron Lett.*, 2003, **44**, 6871.
12 A. Yamane, *Nucleic Acids Res.*, 2002, **30**, e97.
13 U. B. Christensen and E. B. Pedersen, *Nucleic Acids Res.*, 2002, **30**, 4918.
14 A. Okamoto, K. Kanatani and I. Saito, *J. Am. Chem. Soc.*, 2004, **126**, 4820.
15 Y. Saito, Y. Miyauchi, A. Okamoto and I. Saito, *Chem. Commun.*, 2004, **126**, 1704.
16 Y. Saito, K. Hanawa, K. Motegi, K. Omoto, A. Okamoto and I. Saito, *Tetrahedron Lett.*, 2005, **46**, 7605.
17 G. T. Hwang, Y. S. Seo and B. H. Kim, *Tetrahedron Lett.*, 2004, **45**, 3543.
18 C. Dohno and I. Saito, *ChemBioChem*, 2005, **6**, 1.
19 D. J. Hurley, S. E. Seaman, J. C. Mazura and Y. Tor, *Org. Lett.*, 2002, **4**, 2305.
20 L. Valis, N. Amann and H.-A. Wagenknecht, *Org. Biomol. Chem.*, 2005, **3**, 36.
21 G. T. Hwang, Y. S. Seo and B. H. Kim, *J. Am. Chem. Soc.*, 2004, **126**, 6528.
22 O. Seitz, F. Bergmann and D. Heindl, *Angew. Chem., Int. Ed.*, 1999, **38**, 2203.
23 O. Köhler, D. V. Jarikote and O. Seitz, *ChemBioChem*, 2005, **6**, 69–77.
24 S. M. Freier, R. Kierzek, M. H. Caruthers, T. Neilson and D. H. Turner, *Biochemistry*, 1986, **25**, 3209.
25 J. SantaLucia, *Proc. Natl. Acad. Sci. U. S. A.*, 1998, **95**, 1460.
26 C. F. Bleczinski and C. Richert, *J. Am. Chem. Soc.*, 1999, **121**, 10889.
27 S. Narayanan, J. Gall and C. Richert, *Nucleic Acids Res.*, 2004, **32**, 2901.
28 Z. Dogan, R. Paulini, J. A. Rojas Stütz, S. Narayana and C. Richert, *J. Am. Chem. Soc.*, 2004, **126**, 4762.
29 L. G. Lee, C.-H. Chen and L. A. Liu, *Cytometry*, 1986, **7**, 508.
30 T. L. Netzel, K. Nafisi, M. Zhao, J. R. Lenhard and I. Johnson, *J. Phys. Chem.*, 1995, **99**, 17936.
31 J. Nygren, N. Svanvik and M. Kubista, *Biopolymers*, 1998, **46**, 39.
32 S. Prodhomme, J.-P. Demaret, S. Vinogradov, U. Asseline, L. Morin-Allory and P. Vigny, *J. Photochem. Photobiol., B*, 1999, **53**, 60.
33 N. Svanvik, A. Stahlberg, U. Sehlstedt, R. Sjöback and M. Kubista, *Anal. Biochem.*, 2000, **287**, 179.
34 N. Svanvik, J. Nygren, G. Westman and M. Kubista, *J. Am. Chem. Soc.*, 2001, **123**, 803.
35 J. Isacsson, H. Cao, L. Ohlsson, S. Nordgren, N. Svanvik, G. Westman, M. Kubista, R. Sjöback and U. Sehlstedt, *Mol. Cell. Probes*, 2000, **14**, 321.
36 E. Privat and U. Asseline, *Bioconjugate Chem.*, 2001, **12**, 757.
37 E. Privat, T. Melvin, U. Asseline and P. Vigny, *Photochem. Photobiol.*, 2001, **74**, 532.
38 U. Asseline, M. Delarue, G. Lancelot, F. Toulme, N. T. Thuong, T. Montenay-Garestier and C. Helene, *Proc. Natl. Acad. Sci. U. S. A.*, 1984, **81**, 3297.
39 U. Asseline, N. T. Thuong and C. Helene, *New J. Chem.*, 1997, **21**, 5.
40 J. F. Williams, S. C. Case-Green, K. Mir and E. M. Southern, *Nucleic Acids Res.*, 1994, **22**, 1365.
41 N. E. Broude, T. Sano, C. L. Smith and C. R. Cantor, *Proc. Natl. Acad. Sci. U. S. A.*, 1994, **91**, 3072.
42 L. G. S. Brooker and G. H. Keyes, *J. Am. Chem. Soc.*, 1937, **59**, 74.
43 L. G. S. Brooker, G. H. Keyes and W. W. Williams, *J. Am. Chem. Soc.*, 1942, **64**, 199.
44 R. Lartia and U. Asseline, *Chem.–Eur. J.*, 2006, **12**, 2270–2281.
45 J. R. Carreon, K. P. Mahon and S. O. Kelly, *Org. Lett.*, 2004, **6**, 517.
46 U. Asseline and N. T. Thuong, in *Current Protocols in Nucleic Acid Chemistry*, ed. S. Beaucage, D. E. Bergstrom, G. D. Glick and R. A. Jones, John Wiley & Sons, New York, 2001, pp. 4.9.1–28.
47 R. Lartia and U. Asseline, *Tetrahedron Lett.*, 2004, **45**, 949.
48 C. R. Cantor, M. M. Warshaw and H. Shapiro, *Biopolymers*, 1970, **9**, 1059.
49 B. Kramer, W. Kramer and H. J. Fritz, *Cell*, 1984, **38**, 879.
50 H.-K. Nguyen, P. Auffray, U. Asseline, D. Dupret and N. T. Thuong, *Nucleic Acids Res.*, 1997, **25**, 3059.
51 H. T. Allawi and J. SantaLucia, Jnr, *Nucleic Acids Res.*, 1998, **26**, 4740.
52 N. Peyret, P. A. Seneviratne, H. T. Allawi and J. SantaLucia, Jnr, *Biochemistry*, 1999, **38**, 3468.
53 P. K. Bhattacharya, J. Cha and J. K. Barton, *Nucleic Acids Res.*, 2002, **30**, 4925.
54 E. M. Boon, D. M. Ceres, T. G. Drummond, M. G. Hill and J. K. Barton, *Nat. Biotechnol.*, 2000, **18**, 1096.
55 J. R. Riordan, J. M. Rommens, B.-S. Kerem, N. Alon, R. Rozmahel, Z. Grzelczak, J. Zielenski, S. Lok, N. Plavsic, J.-L. Chou, M. L. Drumm, M. C. Iannuzzi, F. S. Collins and L.-C. Tsui, *Science*, 1989, **245**, 1066.
56 See: www.genet.sickkids.on.ca/cftr.
57 R. P. Iyer, W. Egan, J. B. Regan and S. L. Beaucage, *J. Am. Chem. Soc.*, 1990, **112**, 1253.